Activation of Targets and Accelerator Components at PSI - a Comparison of Simulation and Measurement

D. Kiselev*, D. Schumann, S. Teichmann, M. Wohlmuther,
Paul Scherrer Institut, 5232 Villigen, Switzerland

Abstract

The ring cyclotron at the PSI accelerator facility accelerates protons to 590 MeV with a current of 2 mA at present. The stepwise increase to 3 mA is planned. During normal operation there are main beam loss points at targets, beam dumps and collimators. If the beam strikes material particles are lost due to multiple scattering. Subsequent nuclear reactions lead to the production of activated materials in the components themselves and their surroundings. During shutdown radioactive components have to be removed for disposal or repair. To some extent the removal requires operations done by personnel nearby the activated components. To estimate the personal dose and to plan working procedures, a way to calculate the expected dose is essential. In addition, for later disposal of the radioactive components the nuclide inventory is required by the authorities. The Monte Carlo particle transport code MCNPX coupled to the build-up and decay codes SP-FISPACT, Orihet3 and Cinder'90, as well as the bookkeeping system PWWMBS developed at PSI, are used to calculate the required quantities. Both methods are explained and the results are compared to measurements of different activated components.

ACTIVATION AT THE ACCELERATOR FACILITY AT PSI

The Paul Scherrer Institut (PSI), located between Zürich and Basel, is divided into a West and an East part by the river Aare. The accelerator facilities and the joined experimental hall are in the Western part. The proton beam is produced by a 60 keV ion source and preaccelerated in the Cockroft Walton generator. At 870 keV the protons are transported to Injector 2, a ring cyclotron itself with 4 sector magnets, where they reach an energy of 72 MeV. The proton beam is then injected to the ring cyclotron and accelerated to a final energy of 590 MeV at 2 mA. An upgrade to 3 mA is in progress. After leaving the ring cyclotron the protons pass through Target M and Target E, one behind the other. Both consist of a graphite wheel where muons and pions are produced and are led through beam pipes to the experiments. Behind Target E there is an optional beam dump but under normal operation the beam continues to the target of the spallation neutron source SINQ. This target contains lead where neutrons are produced by spallation and are moderated to thermal and cold neutrons in a D_2O tank and a 25 K D_2 reservoir, respectively. In the future a small fraction of the beam will be directed to another lead target to produce ultracold neutrons (UCN facility). Close to this area there is a hall dedicated to medical applications. This project is called PROSCAN. Since 2007 protons are produced and accelerated to 250 MeV in the cyclotron COMET. Subsequently the protons are degraded to fit the requirements of two gantries as well as OPTIS2, the upgrade of OPTIS. OPTIS is treating eye tumors and uses the 72 MeV proton beam provided by Injector 1. Near the experimental hall there is also an area called WAKA where valuable, already used and activated components are stored for reuse in the future.

Beside the targets there are also collimators, slits, beam diagnostic elements and magnets in the beam line. All these components get activated and are therefore shielded by iron and several layers of concrete during machine operation. In longer lasting maintenance periods the concrete shielding can be removed and it is possible to take out single components by means of a shielded flask. The dose rates on the working platform after shutdown of the beam for a few weeks, are between 100 and 200 μSv/h. When the activated components get removed for replacement they become radioactive waste. Before disposal the Swiss authorities require a complete list of the nuclide inventory. This can be only provided by calculations. In the case that the activated piece has to be repaired or dismantled it is valuable to know the dose rate in advance to plan working procedures. In addition for future facilities and larger installations an estimate of the amount of radioactive waste produced after shutdown of the operation is required by the swiss authorities. Calculations are also needed for the construction of the shielding around planned installations.

SIMULATION OF THE ACTIVATION

Activation is caused by direct irradiation of the 590 MeV protons but also by secondary particle fields. Direct irradiation occurs usually at controlled loss points like targets and collimators. When a high energy proton bombards a medium-heavy nucleus, the nucleus gets highly excited. In particular neutrons but also protons and light ions like ^{4}He are "spalled", i.e. emitted by the nucleus. This nuclear process is called spallation. Besides the secondary particles produced, the former medium-heavy nucleus is altered to a much lighter isotope which can be instable (radioactive). When the secondary particles penetrate the surrounding shielding mainly neutrons (and photons) remain due to the much stronger interaction of the charged particles. After several collisions of the neutrons with the nuclides in the shielding material the neutrons loose energy, i.e. most

* Daniela.Kiselev@psi.ch

of the neutrons shift to energies below 1 MeV. After several times the elastic collision length in the material is penetrated it leads almost to an unique energy spectrum of the neutrons independent of the thickness of the shielding. One important nuclear process of thermal neutrons is the capture by nuclides. The nuclides get excited afterwards and emit a photon. The newly formed nuclides might be radioactive.

At PSI the Monte Carlo transport program MCNPX [1] is used to calculate the activation induced mainly by direct irradiation. It can deal with most elementary particles like neutrons, protons, pions, photons but also with light to heavy ions in its newest version 2.6.f. For the results presented in this proceeding a modified version of MCNPX2.5.0 [2] was used. The modification allows that all elements of the material composition including impurities undergo a nuclear reaction at each collision (subsequently the appropriate weight is applied). This is of advantage when good statistics have to be collected to achieve a reasonable uncertainty. MCNPX requires a dedicated geometry of the interesting component and its environment. This is quite time expensive since the coding of the geometric part requires for each volume the logical combination of all surfaces which has to be defined*. In the present calculation evaluated cross section tables (ENDF-B.VI) are used for neutron energies less than 20 MeV whereas otherwise the Bertini cascade model [3] with the Dresner evaporation code [4] are applied. As output MCNPX provides the neutron fluxes for energies E less than 20 MeV and the production rates of residual nuclides caused by neutrons of energy E larger than 20 MeV or other particles like protons and pions of any energy. Via a Perl script ("activation script" [5]) these results are fed into one of the buildup and decay codes: Cinder'90 [6], SP-FISPACT [7], Orihet3 [8]. These codes need the irradiation and cooling history of the piece of interest as input. They contain the decay properties of most of the isotopes to track their decay chain and produce follow-up radioisotopes. Cinder'90 has a built-in cross section library for neutron capture the other two codes use the EAF2003 [9] library. These cross sections are folded with the neutron flux provided by MCNPX to obtain the production rates for nuclides created by neutrons of $E < 20$ MeV during irradiation. Finally the output contains the nuclide inventory as well as the photon rates from the decaying nuclides. The photon rates grouped in energy bins can be used as photon source in MCNPX. This conversion is done via a Perl script ("gamma script" [10]). Running MCNPX with this photon source as an input, the dose rates can be obtained at the locations chosen. If the dose rates one wants to compare with, were measured in another environment as the component was irradiated, the geometry input needs to be modified.

For calculating the activation of components which were mainly exposed to secondary fields the program PWWMBS (PSI West Waste Management Bookkeeping System) [11] is used at PSI. It was developed at PSI especially for the purpose of obtaining the nuclide inventory of radioactive waste. Therefore it contains a data bank to keep track of the waste already processed. It also contains its own cross section library (PSIMECX) [12, 13] developed at PSI. As input the weight, its material composition and the location during irradiation have to be known. The material composition is chosen from a couple of predefined materials whose composition is the average of some samples taken at PSI. According to the location the appropriate shape of the neutron flux energy spectrum is chosen. The production rates for the residual nuclides are obtained by folding the neutron flux spectrum with the built-in cross sections. PWWMBS also contains parts of the build-up and decay code Orihet3. This allows to calculate the nuclide inventory when the date of the installation and removal of the component is known. The periods of the irradiation and the corresponding current are contained in a database of PWWMBS. The nuclide inventory cannot be calculated in absolute values because the neutron flux energy spectrum contains only relative values. Therefore the nuclide inventory is scaled to the surface dose rate which has to be known, i.e. has to be measured beforehand.

COMPARISON BETWEEN CALCULATION AND MEASUREMENT

In this section four examples are presented with the aim to show a variety of applications of the codes described above and compare their results with measured data. Three applications were calculated with MCNPX, two of them compare calculated with experimental dose rates which were measured by a Geiger-Müller type counter. The nuclide inventory of the samples was measured by the radiochemist group at PSI in collaboration with the Accelerator Mass Spectrometry (AMS) groups in Zürich and Munich. Some radioisotopes can be identified by their gamma spectrum, which is measured in a High-Purity Germanium (HPGe) detector. Beta emitters such as Fe55 and Ni63 require a chemical preparation due to the strong self-absorption of beta radiation. After the quantitative analysis of the chemical process the beta emitters are detected in a liquid scintillator (LSC). Long-lived isotopes have usually a small activity and are therefore counted with AMS or Inductively Coupled Plasma Mass Spectrometry (ICP-MS).

Activation in samples of SINQ-Target 3

The insert of SINQ-Target 3 was mounted in the SINQ facility to produce thermal and cold neutrons. This target was an early trial version and therefore it contains no lead but consists of solid Zircaloy† tubes in a hexadimensional structure. The proton beam impinges on the target from below. It is surrounded by D_2O to moderate the fast neutrons produced by spallation in the target. The target is fixed with Zircaloy screws to the connection tube also filled with

*Although a couple of macrobodies exist the use is not always of advantage and time saving.

†Zircaloy is a high zirconium alloy.

D_2O. Behind it the first part of the shielding made out of 316L steel follows. All three components are surrounded by the double-shell safety hull made of AlMg3 (aluminum with 3% magnesium). The geometrical model for the MCNPX simulation is shown in Fig. 1. Three samples were taken from the insert of target 3. One was from the safety hull which was directly exposed to the proton beam, the other was taken in front of the first shielding and the third sample consists of one of the Zircaloy screws. Target 3 was irradiated by 6.77 Ah from mid of 1998 to the end of 1999 where every year there is a planned shutdown period at PSI lasting from Christmas to mid of April.

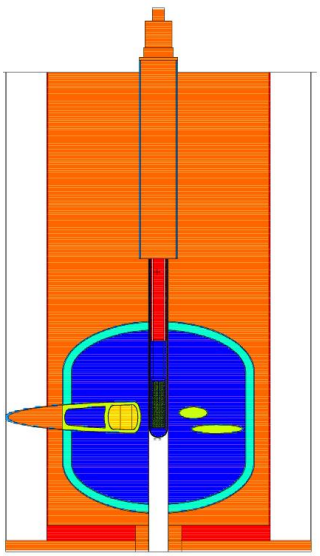

Figure 1: Geometrical model of the SINQ facility used for the calculation in MCNPX. The proton beam hits the target from below.

In figs. 2 and 3 the ratio of the measured to calculated activity in the samples of the steel shielding and the safety hull are presented, respectively [14]. The calculation was performed with MCNPX and Cinder'90 as described in the previous section. In the simulation two different material compositions were used which are represented by the two different columns in the figures. The shaded columns in Fig. 2 result from a material analysis in 1996 whereas the other material composition is an average over 3 samples. For AlMg3 there is a material analysis from 1996 and 2004 available where the first one does not contain natural silver. For details see Table 1. The results for the sample of the steel shielding does not depend strongly on the material compositions used. Overall good agreement between the calculation and the experimental activity is found except for Fe60 where the simulation underpredicts the activity by a factor of eight. This discrepancy was already seen in other samples and seems to be a systematic error either in the measurement or the calculation. In case of the safety hull the second material composition leads to better agreement in particular for Co60 and Ag108m. The reason is that these two isotopes are produced by neutron capture

Table 1: Material composition used in the MCNPX calculation for the safety hull (AlMg3) and the steel shielding (316L). "avg." refers to an average of three material compositions. The values are in weight percentage.

Element	AlMg3 (1996)	AlMg3 (2004)	316L (1996)	316L (avg.)
Ag		4.00E-05		0.0002
Al	96.36	95.95	0.0044	0.0153
Ba		0.000063		
C			0.023	0.023
Ca		0.00122		0.0027
Co		0.00014	0.178	0.1094
Cr	0.037	0.0292	16.8	17.2
Cs				0.0013
Cu	0.03	0.0826	0.361	0.3163
Fe	0.232	0.269	65.7718	65.6041
K		0.0002		0.0001
Mg	2.9	3.204		0.0003
Mn	0.313	0.327	1.71	1.561
Mo		0.00174	2.55	2.4533
Na		0.00006		0.0027
Ni		0.0031	12	12.0666
P			0.022	0.019
Pb		0.00225		
Rb				0.0003
S			0.002	0.0133
Si	0.056	0.03	0.477	0.4463
Sn			0.009	0.0056
Ti	0.013	0.02	0.0346	0.0551
V	0.005	0.00364	0.0522	0.0989
Zn	0.054	0.0463	0.005	

from the natural isotope composition of the element. Because the material composition from 1996 does not contain natural silver Ag108m cannot be produced. This demonstrates how important the correct material composition is and that also impurities have to be known. The material composition is one important source which leads to inaccurate results in the simulation.

In Fig. 3 the simulation overpredicts Na22 by a factor of 10. Using SP-FISPACT instead of Cinder'90 would lead to a ratio of 0.72. This result should not be misinterpreted. First, the three codes Cinder'90, SP-FISPACT and Orihet3 give almost identical results for most of the nuclides. Second, this discrepancy between the two codes in case of Na22 is not always present. For the sample of the steel shielding for example there is only a 20 % difference.

Supporting the planning of a new hot cell at PSI

During the planning phase of a new hot cell at PSI the question arose how thick the outer wall needs to be, which serves as a shielding against a non-controlled area (zone 0). The most activated component at PSI which has to be han-

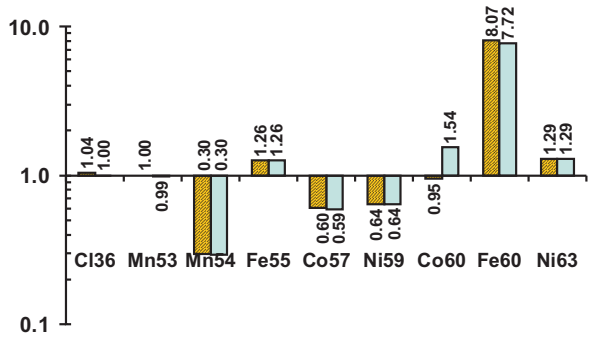

Figure 2: The diagram shows for two different material compositions the ratio of the experimental to calculated activity in the sample of the steel shielding.

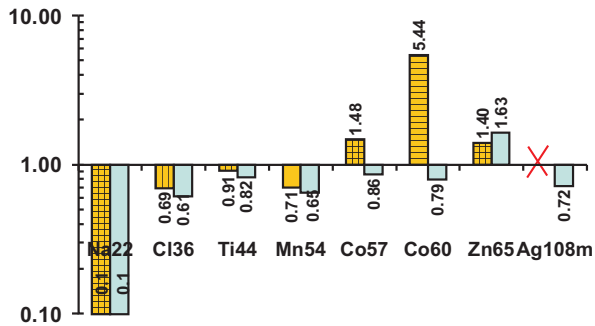

Figure 3: Similar to Fig. 2 but for the sample of the safety hull. Note that for the first material composition no Ag108m is produced in the simulation.

dled regularly in the hot cell[‡], is the SINQ target. Nowadays it consists of lead embedded in Zircaloy tubes. For the case of a 3 mA proton beam in the ring cyclotron[§] which will be available after the upgrade of the facility, and a target operation for 2 years, the nuclide inventory was calculated with MCNPX and Cinder'90. The nuclide inventory was then fed into Microshield [15] to design the shielding. This calculation and the results are not subject of this paper. Here we want to estimate how accurate the predictions are. The shielding calculations depend on the energy spectrum of the gamma radiation. The dose rate is the sum over the gamma spectrum weighted by energy-dose conversion factors. However, the calculated dose rate can be compared to measured values on SINQ targets which were already in use. This was demonstrated for SINQ target 4 which was irradiated for 2 years by 10 Ah in total. After 10 month cool-down the dose rates were measured in front of and along the safety hull at certain positions (M1 to M8 in Fig. 4) in a distance of 3 cm, 30 cm and 100 cm. The SINQ target 4 consisted of steel tubes filled with lead. A target with Zircaloy tubes is currently in use but not yet removed from the SINQ facility. It should be mentioned that the dose rates of a target with Zircaloy tubes are about two times higher than with steel tubes.

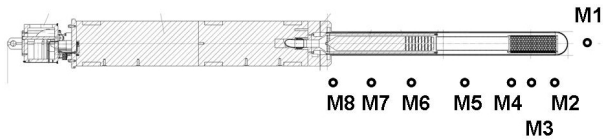

Figure 4: Insert of SINQ target 4 which consists of steel tubes filled with lead. M1 to M8 are the locations where the dose rates were measured at 3 cm, 30 cm and 100 cm distance.

In figs. 5 and 6 the dose rates in Sv/h at a distance of 100 cm and 3 cm distance are shown as a function of the position. The experimental values are indicated by squares, the ones simulated with MCNPX and Cinder'90 by rhombi. At 100 cm distance there is good agreement of the shape but the calculated values underestimate the data by a factor of two in the region of the lead target. We consider this discrepancy as acceptable. At 3 cm distance the comparison looks fine in the region of the target but there is a significant deviation by a factor of 10 in the region of the shielding where the dose rate is two orders of magnitude lower than at the target. The reason is that the measurement was done with a Geiger-Müller tube which is most sensitive to radiation along the tube and almost ignores the photons crossing the tube at an larger angle. This means that in the experiment the device measures mainly the contribution coming from the location where the tube is positioned. This is true particular for small distances. In the simulation the calculated dose rate is equally sensitive to all directions. Since the target region is much higher activated than the area of the shielding, the simulated value exceeds the measured one.

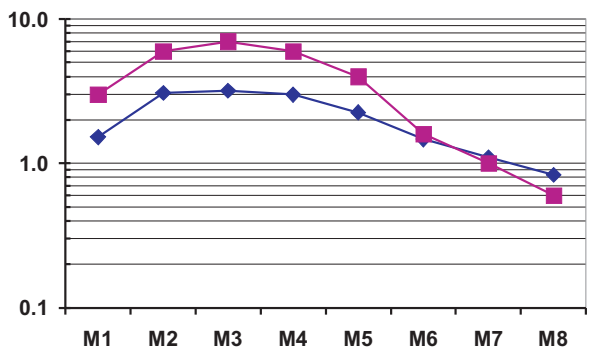

Figure 5: Measured (squares) and calculated (rhombi) dose rates in Sv/h at a distance of 100 cm as a function of the position in front of (M1) and along the target4 (M2 – M8).

[‡]In exceptional cases and for very high activated components a temporary shielding can be installed.

[§]It should be noted that the current on the SINQ target is about 30 % smaller due to absorption in the 4 cm thick graphite target E.

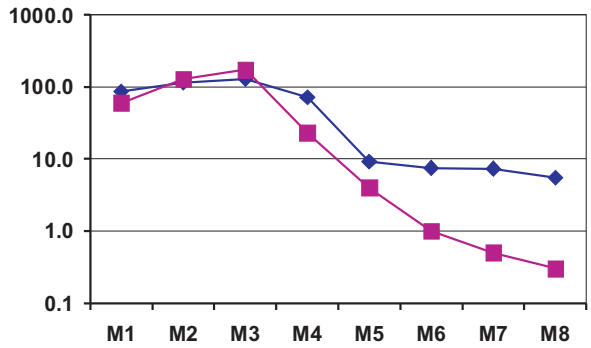

Figure 6: Same as Fig. 5 but for a distance of 3 cm.

Dose rate mapping at the PIREX beam line

The PIREX (Proton Irradiation Experiment) beam line was in operation from 1988 to 2004 and received 20 μA beam from the main 590 MeV proton beam via an electrostatic splitter foil. In the setup of the PIREX experiments which consisted of three vacuum chambers, samples were irradiated for the purpose of testing materials on their radiation hardness. Alternatively the beam could also be delivered to the radiotherapy station Gantry I using a degrader system to reduce the beam energy and intensity. In 2006 the PIREX beam line had to be dismantled to free space for the new UCN hall. Due to the installation of COMET the PIREX beam line got obsolete. For a better planning of this work a few dose rates were measured and a complete map of dose rates was calculated for the third vacuum chamber which is activated the most [10]. The third vacuum chamber consisted of three sections where in the first one the beam monitor was mounted, in the second one the degrader made out of copper and carbon disks. The last section contained the copper beam dump. When the beam was delivered to Gantry I the beam dump was out of beam and the degrader in.

The geometrical model used in the MCNPX calculation is shown in Fig. 7 where the three sections are indicated. The proton beam enters from the right 1.5 m above the concrete floor. All three vacuum chambers were made out of stainless steel and shielded on the side and on the top with steel blocks of 2 m thickness. In the simulation the assumption was made that the degrader and the beam dump were always in the beam at the same time because no record exists on the position of the degrader/beam dump as a function of time. Further the irradiation history was simplified in the sense that an averaged current of 8.3 μA over 16.6 y was used. After 2.3 y the dose rates were measured in the locations marked by the capital letters in Fig. 7. The calculation of the dose rates was performed with MCNPX2.5.0 and SP-FISPACT using the EAF2003 cross sections. The gamma spectrum was calculated for each of the 225 cells and then used as gamma source in a follow up MCNPX run. A MESH tally was applied to visualize the remanent dose field present around the vacuum chamber. At certain

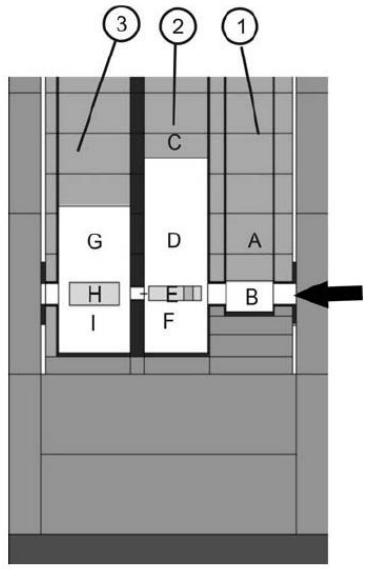

Figure 7: Geometrical model (vertical cut) of the third vacuum chamber of PIREX as used in MCNPX. The proton beam enters from the right and passes through the beam current monitor, the degrader (if in beam) and is stopped in the beam dump (if in place). The letters indicate the locations where the dose rates were measured.

locations where the dose rates were measured, point tallies were used. These results compared to the measured values are shown in Table 2 at the locations A to I as indicated in Fig. 7.

Table 2: Comparison of the measured and calculated dose rates of the third vacuum chamber at the locations indicated in Fig. 7.

Points	Measured dose rate (Sv/h)	Calculated dose rate (Sv/h)	Ratio (C/M)
A	0.115	0.181	1.57
B	0.230	0.255	1.11
C	0.020	0.057	2.85
D	0.350	0.434	1.24
E	1.000	0.529	0.53
F	0.700	0.501	0.72
G	0.300	0.279	0.93
H	0.660	0.315	0.48
I	0.380	0.295	0.78

In general there is good agreement between the measured and calculated dose rates in the third vacuum chamber of PIREX. All values are within a factor of 2 with two exceptions at C and H. For C there is an uncertainty in the location where the measurement was done. The discrepancy at H arises from the simplified assumption in the simulation that both the degrader and the beam dump were always in the beam. However, when the irradiation experiments of PIREX were performed the beam dump was in

but the degrader was out. That means that almost the full beam current ($\approx 20\,\mu$A) was stopped in the beam dump and not only the few nA after passing through the degrader. Therefore in reality the beam dump is more activated and the simulation underpredicts the measured value.

Activation of samples in the μE4 beamline

The μE4 beamline is one out of five beamlines around Target E for the purpose of extracting muons and pions produced in the proton-carbon reaction in Target E. In 2004/2005 the μE4 beamline was rebuilt to increase the acceptance for muons of momentum 28 MeV/c [16] which are produced at the surface of target E. In 2004 the old beamline was dismantled and several samples were taken to measure the activity of a couple of radioisotopes. The samples were obtained by drilling holes into the components of interest and collecting the borings for further analysis. Samples were taken from the entry and exit of the vacuum chamber (beam tube) of the bending magnet ASK 61, from the shielding of the shutter and from the shutter itself located behind ASK 61. The magnet ASK 61 is the first bending magnet in the μE4 beamline which start at an angle of 90 ^{o} to the proton beamline. The distance between ASK 61 and the proton beam line is approximately 3 m. Therefore the components were activated not by direct irradiation of the proton beam but in secondary fields and the calculation of the nuclide inventory can be performed with PWWMBS. According to their location an appropriate neutron flux spectrum was chosen. In the following we want to concentrate on the results of the sample from the beam tube in front of ASK 61. The beam tube was made out of stainless steel and irradiated over 13 years, from August 1991 to December 2003. End of February 2004 the γ-radiation of the samples was measured using a Ge detector. Due to the short time between the end of the irradiation and making the analysis many of the short half-life nuclides could be measured. Later, in 2004 and 2005 longer half-life nuclide were counted by AMS (Al26, Cl36) and the β radiation of Ni63 and Fe55 were detected by LSC.

In Fig. 8 the ratio of the experimental to calculated activity is shown for 18 radioisotopes in the sample from the beam tube in front of ASK 61 [17, 18]. The overall agreement is satisfactory. However, Cl36 is overestimated by a factor of about 60 by the calculation. The main production mechanism of Cl36 is due to low energy neutron capture of Cl35. The discrepancy can be likely explained by a too high content of Cl35 in the material composition of stainless steel used by PWWMBS. This again emphasizes the importance of knowing the exact material composition which is in practice impossible.

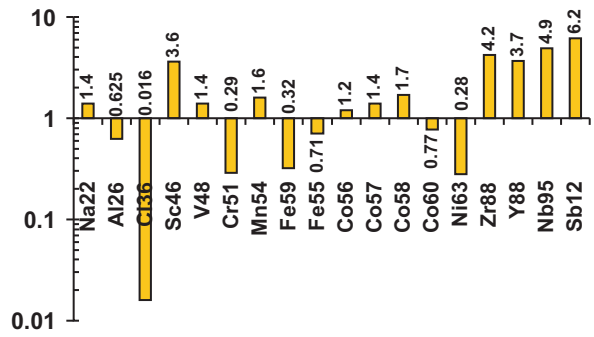

Figure 8: Ratio of the measured to calculated activity of the sample taken at the beam tube in front of the bending magnet ASK 61. The calculations were done with PWWMBS using a standard material composition.

RADIOACTIVE WASTE AT PSI

After removal of the bending magnet ASK 61 from the beam line it became radioactive waste and therefore went into a waste container made out of concrete. The waste containers have a base area of 1.5 m times 1.5 m and are 2 m high. The wall thickness is 12 cm or 30 cm depending on the dose rate of the components. Sometimes additional shielding has to be used inside the container. Besides magnets also collimators, beam diagnostic elements, vacuum chambers, shielding and electrical installations are regularly separated at PSI for disposal. Targets are disposed separately. The filled containers are stored in a temporary storage building. For the final conditioning they have to be filled with special concrete which can fill all accessible voids. The total activity per container is typical between 10^{10} and 10^{13} Bq. The average weight of the waste filled into the container is 4.5 t. At PSI three to four containers are filled per year. Fig. 9 shows an average the composition of the materials in the containers. The sum of the data is normalized to 100 %. Almost 80 % of the components there consist of normal and stainless steel. This is followed by concrete and cast iron.

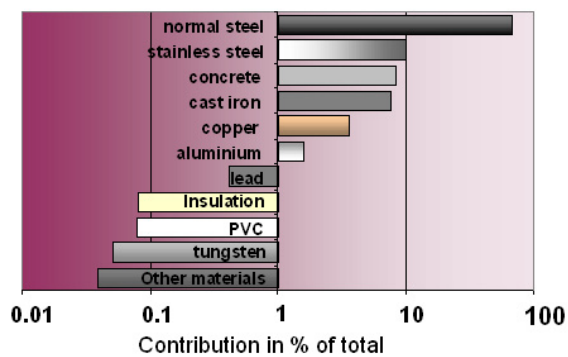

Figure 9: Percentage of materials filled in containers for waste disposal (averaged values).

COMPARISON BETWEEN MCNPX AND PWWMBS

As it was stated in the beginning, PWWMBS and MCNPX can be both used for nuclide inventory calculations but their field of application is different. PWWMBS is used mainly for calculating the nuclide inventory in components which were activated in secondary particle fields. This is the case for most of the components ending up as radioactive waste in the containers. On the other hand MCNPX is applied for components directly irradiated by the proton beam. While PWWMBS needs a measured surface dose rate MCNPX in combination with build-up and decay programs can be also used for predicting remanent dose rates ¶. However, for most applications MCNPX needs an elaborate geometry as input which describes not only the component of interest but also its environment. The latter can influence the particle energy spectrum. This requires large cpu times (typical 10 h on 256 cores) and sometimes leads to statistical limitations on the production of seldomly produced radioisotopes. Due to the folding of a predefined neutron energy spectrum with cross sections PWWMBS suffers not from statistical errors. Further advantages are that the program is user friendly and the results are obtained fast due to the simplifications made in the code. With respect to the amount of waste coming from many different locations these are a great advantages. Moreover, the dose rate of the personnel is minimized because only the dose rate has to be measured (at very activated pieces by the manipulator in the hot cell). No samples from each component are required which also would lead to the risk of contaminating the surrounding. The accuracy of the radioisotopes which could be measured up to now, is about a factor of 10 with few exceptions. Using MCNPX the accuracy in the prediction of the activity of most of the radioisotopes is about a factor of three while the calculated dose rate agrees with the measured one within a factor of two.

SUMMARY

Due to the need of declaring all radioisotopes of an activated component to be disposed as radioactive waste for disposal, predictions via calculations are unavoidable. In addition these codes help to estimate the amount of waste produced in future facilities. At PSI PWWMBS is used for most of the radioactive waste exposed to secondary particle fields. MCNPX coupled to the decay codes Orihet3, Cinder'90 and SP-FISPACT is able not only to calculate the nuclide inventory but also the remanent dose rate. This is valuable for planning of work procedures or estimating the thickness of shielding.

In this paper four examples were chosen to show the applicability of these codes but also their limitations. The results, dose rates and the nuclide inventory, were compared to measured values. In general the agreement is good. Using MCNPX the dose rates are predicted within a factor of two and the activities of the radioisotopes are within a factor of three. With PWWMBS the accuracy is about a factor of 10 for the nuclide inventory. However there are still some larger discrepancies; the reasons are not always understood because of the complexity of the problem. Therefore it is important to continue the comparison between the codes and the measurements to acquire a large data base. This will help to tackle down problems. In the future it is also planned to use beside the Bertini/Dresner model more recent implementations in MCNPX: the Liège intranuclear cascade (INCL4 [19]) combined with the evaporation/fission code ABLA (abrasion-ablation model [20]) as well as the Cascade-Exciton Model (CEM03 [21]). It is expected that this will further improve the results.

¶MCNPX can be exploited for many other applications. In our group it is also applied to calculate energy deposit and neutronics (SINQ). The energy deposit is fed into further codes to get the temperature and stress distribution.

ACKNOWLEDGEMENT

We would like to thank F. Atchison for developing the program PWWMBS and committing it to us. Also we want to express our thanks to the AMS groups at ETH-Hönggerberg (V. Alfimov, P. Kubik, H.-A. Synal) and at TU München (Th. Faestermann, G. Korschinek, G. Rugel) for providing us with the data of many radioisotopes. Further we want to thank O. Morath from the dosimetry and radiation protection group at PSI for measuring the dose rates and discussing the results.

REFERENCES

[1] D. Pelowitz, ed., MCNPX Users Manual, Version 2.5.0, LA-CP-05-0369, Los Alamos, 2005.

[2] M. Wohlmuther, F.X. Gallmeier, M. Brugger and S. Roesler, "Activation of Trace Elements and Impurities - A new Ansatz for Monte Carlo Calculation", Proc. of the 11th Int. Conf. on Radiation Shielding and 15th Topical Meeting of the Radiation Protection and Shielding Division of ANS, Georgia, USA, 2008.

[3] H. W. Bertini, Phys. Rev 131 (1963) 1801. H. W. Bertini, Phys. Rev. 188 (1969) 1711.

[4] L. Dresner, "EVAP-A Fortran Program for Calculating the Evaporation of Various Particles from Excited Compound Nuclei", Oak Ridge National Laboratory report ORNL-TM-7882 (July 1981).

[5] F.X. Gallmeier et al.,"An Environment using Nuclear Inventory Codes in Combination with the Radiation Transport Code MCNPX for Accelerator Activation Problem", Proc. of the 8th Int. Topical Meeting on Nuclear Applications and Utilization of Accelerators, Pocatello, Aug. 2007, S. 207.

[6] W.B. Wilson et al., "Recent Developments of the CINDER'90 Transmutation Code and Data Library for Actinide Transmutation Studie", Proc. GLOBAL'95 Int. Conf. on Evaluation of Emerging Nuclear Fuel Cycle Systems, Versailles, France, 1995.

[7] R.A. Forrest, M.R. Gilbert, "FISPACT-2003: User manual", Culham Report UKAEA FUS 485, 2002.
C. Petrovich, "SP-FISPACT 2001: A computer code for

activation and decay calculations for intermediate energies. A connection of FISPACT to MCNP", RT/ERG/2001/10, ENEA Bologna, 2001.

[8] F. Atchison, H. Schaal, "ORIHET3-Version 1.12, A Guide for Users", 2001.

[9] R.A. Forrest, Culham Report UKAEA FUS 484, 2002.

[10] M. Wohlmuther, B.J. Micklich, F.X. Gallmeier, S. Forss, R. Kueng, O. Morath: "Calculation of remanent dose distribution with MCNPX", Proc. of the 8th Int. Topical Meeting on Nuclear Applications and Utilization of Accelerators, Pocatello, Aug. 2007, S. 226.

[11] F. Atchison, "PWWMBS: A computer based book-keeping system for radioactive waste from PSI-West accelerator complex", internal PSI report AN-96-01-20, PSI, 2001.

[12] F. Atchison, "The PSIMECX medium-energy neutron activation cross section library", Parts I, II, III, IV, PSI Reports 98-09, 98-10, 98-11, 98-12 (1998).

[13] F. Atchison, Nucl. Instr. Meth. B 259 (2007) 909.

[14] D. Kiselev, D. Schumann, S. Teichmann, M. Wohlmuther, "Berechnung des Nuklidinventars von drei Proben aus dem SINQ-Target 3", internal PSI report TM-85-08-03, PSI, 2008.

[15] Microshield, Version 6, Users Manual, Grove Engineering, March 2003.

[16] T. Prokscha et al., Nucl. Instr. Meth. (2008), in press.

[17] F. Atchison, D. Schumann, R.Weinreich, "Comparison of PWWMBS calculated inventories with sample analysis result", internal PSI report TM-85-94-16, PSI, 2004.

[18] M. Wohlmuther, internal PSI memo, PSI, 2005.

[19] A. Boudard, J. Cugnon, S. Leray, C. Volant, Phys. Rev. C 66 (2002) 044615.

[20] A.R. Junghans, M. de Jong, H.-G. Clerc, A.V. Ignatyuk, G.A. Kudyaev, K.-H. Schmidt, Nucl. Phys. A 629 (1998) 635.

[21] S.G. Mashnik, M.I. Baznat, K.K. Gudima, A.J. Sierk, R.E. Prael, J. Nuc. Radiochem. Sci. 6 (2005) A1.